PROCEEDINGS OF SCIENCE

Complete nucleosynthesis calculations for low−mass stars from NuGrid

M. Pignatari*[abc], F. Herwig[abd], M. E. Bennett[ad], S. Diehl[aef], C. L. Fryer[af], R. Hirschi[abg], A. Hungerford[af], G. Magkotsios[ach], G. Rockefeller[af], F. X. Timmes[ah], and P. Young[ah]

[a] *The NuGrid Collaboration*
[b] *Astrophysics Group, Keele University, ST5 5BG, UK*
[c] *Joint Institute for Nuclear Astrophysics, University of Notre Dame, IN, 46556, USA*
[d] *Dept. of Physics & Astronomy, Victoria, BC, V8W 3P6, Canada*
[e] *Theoretical Astrophysics Group (T-6), Los Alamos National Laboratory, Los Alamos, NM, 87544, USA*
[f] *Computational Methods (CCS-2), Los Alamos National Laboratory, Los Alamos, NM, 87544, USA*
[g] *IPMU, University of Tokyo, Kashiwa, Chiba 277-8582, Japan*
[h] *School of Earth and Space Exploration, Arizona State University, Tempe, AZ 85287, USA*
E-mail: marco@astro.keele.ac.uk

Many nucleosynthesis and mixing processes of low−mass stars as they evolve from the Main Sequence to the thermal-pulse Asymptotic Giant Branch phase (TP−AGB) are well understood (although of course important physics components, e.g. rotation, magnetic fields, gravity wave mixing, remain poorly known). Nevertheless, in the last years presolar grain measurements with high resolution have presented new puzzling problems and strong constraints on nucleosynthesis processes in stars. The goal of the NuGrid collaboration is to present uniform yields for a large range of masses and metallicities, including low−mass stars and massive stars and their explosions. Here we present the first calculations of stellar evolution and high−resolution, post−processing simulations of an AGB star with an initial mass of 2 $M_{\odot}$ and solar−like metallicity (Z=0.01), based on the post−processing code *PPN*. In particular, we analyze the formation and evolution of the radiative ^{13}C−pocket between the 17th TP and the 18th TP. The *s*-process nucleosynthesis profile of a sample of heavy isotopes is also discussed, before the next convective TP occurrence.

10th Symposium on Nuclei in the Cosmos
July 27 - August 1 2008
Mackinac Island, Michigan, USA

*Speaker.

1. Introduction

When He−burning is exhausted in the core, low mass stars (1.5 − 3 $M_{\odot}$) evolve along the AGB. Late on the AGB, recurrent thermal instabilities called Thermal Pulses (TP-AGB phase, [16]) affect shell He−burning history. After TPs (time scale in the order of few hundreds years), the third dredge−up events (TDU) mix He shell material in the envelope, and fresh protons down in the He−intershell. A ^{13}C−pocket is formed in the radiative He intershell phase, where the ^{13}C(α,n)^{16}O neutron source becomes efficient activating slow neutron capture process (s−process, [4]). A marginal contribution is also given by the partial activation of the ^{22}Ne(α,n)^{25}Mg at the bottom of the He intershell (e.g., [8]).
As a result of the TDU enriching the AGB envelope with *s*-process rich material, AGB stars provide most of the s elements beyond Sr observed in the Solar System. In particular, the "main component" between Sr and Pb is produced by solar−like AGB stars, while the "strong component" explaining half of the solar ^{208}Pb is produced by low metallicity AGB stars ([2], and references therein). Carbon is also dredged-up with s elements in the envelope, and eventually the AGB star may become a C-rich star (C(N) star), meaning that carbon is more abundant than oxygen in the envelope.
Spectroscopic observations and composition measurements in presolar grains formed in AGB stars confirm this scenario ([5],[12] ,respectively), and provide important insight to study and understand those stars in more details. In particular, presolar grains carry the isotopic and chemical signature of their parent stars (e.g., [18],[12], [3]), providing a powerful tool to test and constrain stellar models and nuclear physics inputs. The *NuGrid* project (see also Herwig et al. in this volume) has the goal to generate uniform yields for a large range of masses and metallicities also for low−mass stars, and to constrain them with observations. In this proceeding we present the first calculations of stellar evolution and high-resolution, post-processing simulations of a 2 $M_{\odot}$ Z = 0.01 AGB star, based on the post−processing code *PPN*.

2. Post−processing calculations

The main input parameters for the post-processing calculations are given by a 2 $M_{\odot}$ and Z = 0.01 star (EVOL Code, e.g., [10]). The stellar model has been calculated assuming an overshoot parameter f = 0.128 at the bottom of the envelope and f = 0.008 for all the other convective boundaries. The f applied at the base of the convective TP in the He shell (f = 0.008) has been constrained to explain the He/C/O ratio observed in H deficient post-AGB stars of type PG1159 and in WC central stars of planetary nebulae ([17]). The higher overshoot parameter at the bottom of the envelope is calibrated to reproduce the mass of the ^{13}C-pocket needed to reproduce the observed overabundance of *s*-process elements [13]. The post-processing code *PPN* is described in Herwig et al. (this vol.) and includes dynamically all species from H to Bi. Concerning the simulations shown in this proceeding, from the physics package in *PPN* we selected [1] (NACRE compilation) for the main charged particle reactions, [6] (Kadonis compilation) for neutron capture reactions and [15] for unstable isotopes not included in the Kadonis network. We selected [14] and [7] (or terrestrial rates if not available in the previous references) for stellar β-decay rates of light unstable isotopes, and [9] (or terrestrial rates if not available) for β-decay rates of heavy

unstable isotopes (see also Herwig et al. in this volume for more details about the physics package).

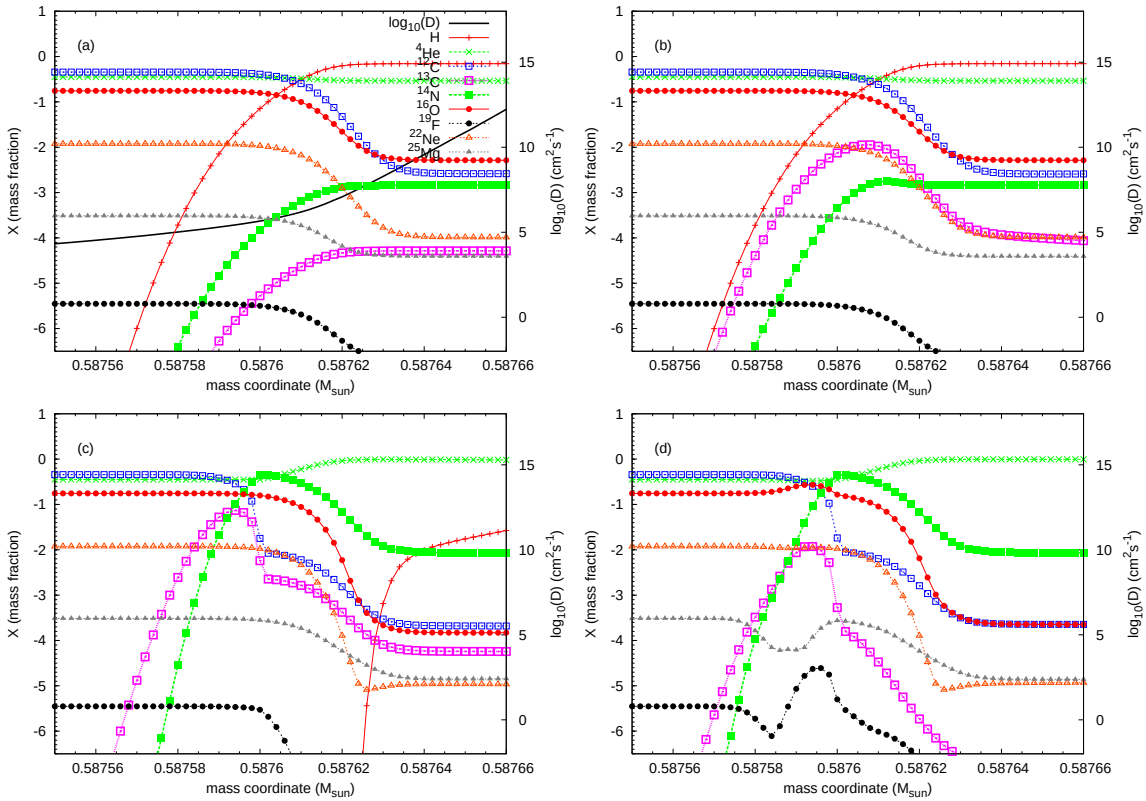

Figure 1: Panel (a,b,c,d): Formation and evolution of the ^{13}C-pocket after the 17th TP for the 2 $M_{\odot}$ Z = 0.01 star. The profile for the mixing coefficient D (it is different from zero only in Panel (a)) and for a sample of light isotopes is provided.

In Fig. 1 we show the formation and evolution of the ^{13}C-pocket between the 17th TP and the 18th TP (interpulse phase of about 70000 yr). In Panel (a) the TDU mixes down in the He intershell protons and envelope material, before the re-activation of the H shell. In Panel (b) the abundant ^{12}C is efficiently capturing protons producing ^{13}C in radiative conditions via the nucleosynthesis channel ^{12}C(p,γ)^{13}N(β^+)^{13}C (e.g., [8]). At the ^{13}C abundance peak, also ^{14}N starts to be produced by the proton capture channel ^{13}C(p,γ)^{14}N. In Panel (c) the ^{13}C-pocket final shape is shown, since protons are fully consumed. The pocket size is $1-2\times10^{-5}$ $M_{\odot}$. Moving outward, a prominent ^{14}N-

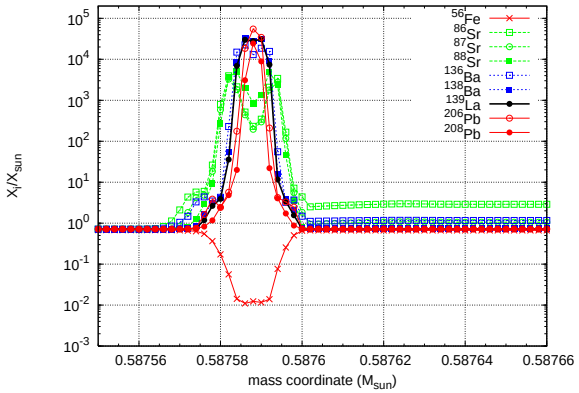

Figure 2: The overabundances of a sample of heavy isotopes has been reported (among them the s-only isotopes ^{86,87}Sr, ^{136}Ba and ^{206}Pb), at the same time-step of Fig. 1, Panel (d).

pocket is formed just after the ^{13}C-pocket, as expected. After about 40000 years, the temperature in the ^{13}C-pocket is high enough to efficiently activate the ^{13}C(α,n)^{16}O reaction, producing neutrons for the *s* process. In Panel (d) we show the ^{13}C-pocket region once ^{13}C has been burnt and the *s* process is not anymore efficient. ^{25}Mg is the main neutron poison in the ^{13}C-pocket, and it has been partially depleted by the neutron flux. In the ^{14}N-pocket, instead, as it is well known ^{14}N(n,p)^{14}C is the main neutron poison and the neutron capture efficiency of ^{25}Mg (and of the main *s*-process seed ^{56}Fe) quickly decreases with increasing the ^{14}N abundance. The final ^{19}F abundance profile basically follows the ^{13}C profile. If ^{13}C is more abundant than ^{14}N, then ^{19}F is depleted by neutron capture and by α capture. In case ^{14}N is more abundant than ^{13}C, ^{19}F can be produced starting from ^{14}N [11].
Finally, in Fig. 2, we report the final overabundance profile in the ^{13}C-pocket region for a sample of isotopes at the Sr neutron magic peak (^{86,87,88}Sr), at the Ba neutron magic peak (^{136,138}Ba, ^{139}La) and at the Pb neutron magic peak (^{206,208}Ba). The *ls* peak species (e.g. Sr, [5]) show a maximum of overproduction of about 5×10^3, while the *hs* peak (e.g. Ba) and the Pb peak show an overproduction of about few 10^4. Sr isotopes show a double peak in coincidence of the ^{56}Fe depletion tails. At 0.58758 $M_\odot$ the ^{13}C abundance is rapidly decreasing and as a consequence a lower amount of neutrons are produced. On the other hand, at 0.587595 $M_\odot$ the poisoning effect of ^{14}N is increasing, until the ^{56}Fe neutron capture efficiency is negligible. The Ba peak and the Pb peak are more produced in the center of the ^{13}C-pocket, where lighter Sr peak elements are feeding *s* nucleosynthesis of heavier elements. The next convective TP will mix the *s*-process rich pocket in all the He intershell, which will be partially dredged up in the envelope by the next TDU event.

The analysis presented Fig. 1 and in Fig. 2 shows part of the capabilities of the *PPN* post-processing code applied to AGB nucleosynthesis calculations. At present, we may calculate the abundances from H to Bi (including isotopic ratios) at any position and at any time in a complete stellar track. Furthermore, in the nuclear network every reaction rate may be automatically chosen between different nuclear sources, or a multiplication factor can be applied or the reaction may be not considered. This opens up possibilities to systematically take into account the effect of nuclear reaction rate uncertainties in our nucleosynthesis calculations.

Acknowledgments

M.P. acknowledges support through NSF grants PHY 02-16783 (JINA). M.P. and F.H. were supported by a Marie Curie International Reintegration Grant MIRG-CT-2006-046520 within the European FP6.

References

[1] C. Angulo, M. Arnould, M. Rayet, P. Descouvemont, D. Baye, C. Leclercq-Willain, A. Coc, S. Barhoumi, P. Aguer, C. Rolfs, R. Kunz, J. W. Hammer, A. Mayer, T. Paradellis, S. Kossionides, C. Chronidou, K. Spyrou, S. Degl'Innocenti, G. Fiorentini, B. Ricci, S. Zavatarelli, C. Providencia, H. Wolters, J. Soares, C. Grama, J. Rahighi, A. Shotter, and M. Lamehi Rachti, *A compilation of charged-particle induced thermonuclear reaction rates.*, Nuclear Physics A **656** (1999), 3–183.

[2] C. Arlandini, F. Käppeler, K. Wisshak, R. Gallino, M. Lugaro, M. Busso, and O. Straniero, *Neutron Capture in Low-Mass Asymptotic Giant Branch Stars: Cross Sections and Abundance Signatures*, ApJ**525** (1999), 886–900.

[3] J. G. Barzyk, M. R. Savina, A. M. Davis, R. Gallino, M. J. Pellin, R. S. Lewis, S. Amari, and R. N. Clayton, *Multi-element isotopic analysis of single presolar SiC grains*, New Astronomy Review **50** (2006), 587–590.

[4] E. M. Burbidge, G. R. Burbidge, W. A. Fowler, and F. Hoyle, *Synthesis of the Elements in Stars*, Reviews of Modern Physics **29** (1957), 547–650.

[5] M. Busso, R. Gallino, D. L. Lambert, C. Travaglio, and V. V. Smith, *Nucleosynthesis and Mixing on the Asymptotic Giant Branch. III. Predicted and Observed s-Process Abundances*, ApJ**557** (2001), 802–821.

[6] I. Dillmann, R. Plag, M. Heil, F. Käppeler, and T. Rauscher, *Present status of the KADoNiS database*, International Symposium on Nuclear Astrophysics - Nuclei in the Cosmos, 2006.

[7] G. M. Fuller, W. A. Fowler, and M. J. Newman, *Stellar weak interaction rates for intermediate-mass nuclei. IV - Interpolation procedures for rapidly varying lepton capture rates using effective log (ft)-values*, ApJ**293** (1985), 1–16.

[8] R. Gallino, C. Arlandini, M. Busso, M. Lugaro, C. Travaglio, O. Straniero, A. Chieffi, and M. Limongi, *Evolution and Nucleosynthesis in Low-Mass Asymptotic Giant Branch Stars. II. Neutron Capture and the s-Process*, ApJ**497** (1998), 388–+.

[9] S. Goriely, *Uncertainties in the solar system r-abundance distribution*, A&A**342** (1999), 881–891.

[10] F. Herwig, S. M. Austin, and J. C. Lattanzio, *Nuclear reaction rate uncertainties and astrophysical modeling: Carbon yields from low-mass giants*, Phys. Rev. C**73** (2006), no. 2, 025802–+.

[11] A. Jorissen, V. V. Smith, and D. L. Lambert, *Fluorine in red giant stars - Evidence for nucleosynthesis*, A&A**261** (1992), 164–187.

[12] M. Lugaro, A. M. Davis, R. Gallino, M. J. Pellin, O. Straniero, and F. Käppeler, *Isotopic Compositions of Strontium, Zirconium, Molybdenum, and Barium in Single Presolar SiC Grains and Asymptotic Giant Branch Stars*, ApJ**593** (2003), 486–508.

[13] M. Lugaro, F. Herwig, J. C. Lattanzio, R. Gallino, and O. Straniero, *s-Process Nucleosynthesis in Asymptotic Giant Branch Stars: A Test for Stellar Evolution*, ApJ**586** (2003), 1305–1319.

[14] T. Oda, M. Hino, K. Muto, M. Takahara, and K. Sato, *Rate Tables for the Weak Processes of sd-Shell Nuclei in Stellar Matter*, Atomic Data and Nuclear Data Tables **56** (1994), 231–+.

[15] T. Rauscher and F.-K. Thielemann, *Astrophysical Reaction Rates From Statistical Model Calculations*, Atomic Data and Nuclear Data Tables **75** (2000), 1–2.

[16] M. Schwarzschild and R. Härm, *Thermal Instability in Non-Degenerate Stars.*, ApJ**142** (1965), 855.

[17] K. Werner and F. Herwig, *The Elemental Abundances in Bare Planetary Nebula Central Stars and the Shell Burning in AGB Stars*, PASP**118** (2006), 183–204.

[18] E. Zinner, *Stellar Nucleosynthesis and the Isotopic Composition of Presolar Grains from Primitive Meteorites*, Annual Review of Earth and Planetary Sciences **26** (1998), 147–188.